

Effect of pore occupancy on the acoustic properties of zeolitic imidazolate framework (ZIF)-8: A Brillouin spectroscopic study at ambient and low temperatures

Dhanya Radhakrishnan and Chandrabhas Narayana

Citation: *The Journal of Chemical Physics* **143**, 234703 (2015); doi: 10.1063/1.4937763

View online: <http://dx.doi.org/10.1063/1.4937763>

View Table of Contents: <http://scitation.aip.org/content/aip/journal/jcp/143/23?ver=pdfcov>

Published by the **AIP Publishing**

Articles you may be interested in

[Guest dependent Brillouin and Raman scattering studies of zeolitic imidazolate framework-8 \(ZIF-8\) under external pressure](#)

J. Chem. Phys. **144**, 134704 (2016); 10.1063/1.4945013

[The elastic constants and related properties of the epsilon polymorph of the energetic material CL-20 determined by Brillouin scattering](#)

J. Chem. Phys. **131**, 214501 (2009); 10.1063/1.3244981

[Acoustic anisotropy in uniaxial tungsten bronze ferroelectric single crystals studied by Brillouin light scattering](#)

J. Appl. Phys. **104**, 104105 (2008); 10.1063/1.3021107

[The elastic constants and related properties of \$\beta\$ -HMX determined by Brillouin scattering](#)

J. Chem. Phys. **122**, 174701 (2005); 10.1063/1.1883627

[Influence of the microstructure on the macroscopic elastic and optical properties of dried sonogels: A Brillouin spectroscopic study](#)

J. Appl. Phys. **81**, 7739 (1997); 10.1063/1.365383



NEW Special Topic Sections

NOW ONLINE
Lithium Niobate Properties and Applications:
Reviews of Emerging Trends

AIP | Applied Physics
Reviews

Effect of pore occupancy on the acoustic properties of zeolitic imidazolate framework (ZIF)-8: A Brillouin spectroscopic study at ambient and low temperatures

Dhanya Radhakrishnan and Chandrabhas Narayana^{a)}

Chemistry and Physics of Materials Unit, Jawaharlal Nehru Centre for Advanced Scientific Research, Jakkur, Bangalore 560064, India

(Received 1 August 2015; accepted 20 November 2015; published online 17 December 2015)

Brillouin spectroscopy is used to study the effect of pore occupancy on the elastic constants by incorporating various guest molecules into zeolitic imidazolate framework (ZIF)-8. A systematic study on the effect of mass and polarizability of the guest has been carried out by incorporating alcohols of varying chain lengths at room temperature. The interaction between the guest and host affects the elastic properties, lifetimes and guest dynamics inside the pores. The elastic anisotropy was seen to reduce upon incorporation of the guests. We have also studied the temperature dependence of the acoustic modes on gas adsorption to understand the framework flexibility. The Brillouin shift of the acoustic modes increases upon temperature dependent gas adsorption with transverse acoustic modes exhibiting a larger shift. This suggests a hardening of otherwise low shear modulus of ZIF-8. Our findings give insight into the role of guest molecules and temperature in tuning the elastic properties of ZIF-8 which is important for practical applications. © 2015 AIP Publishing LLC. [<http://dx.doi.org/10.1063/1.4937763>]

I. INTRODUCTION

Metal organic frameworks (MOFs) are microporous materials consisting of metal ions and organic linkers which have a huge variety of applications ranging from gas storage to drug delivery.^{1,2} Though knowledge of elastic properties of MOFs is very important due to their technological applications, they are rarely studied.³ MOFs exhibit huge responses to external stimuli like temperature, pressure, and guest incorporation due to the presence of weak chemical bonding and flexible organic ligands.⁴ Yet, thorough experimental and computational studies on the elastic properties of MOFs under extreme conditions (temperature/pressure) with or without the presence of guest remain unexplored. To our knowledge, the only study on the temperature dependence of the elastic properties is the molecular dynamics calculations on MOF-5 in the absence of any guest.⁵ Nanoindentation has been used at the ambient temperature to study the influence of guest incorporation on the mechanical properties of some zeolitic imidazolate frameworks (ZIFs), MOF-74-Zn, and a few soft porous crystals, but the temperature dependence of elastic properties on guest incorporation has not been attempted.⁶⁻⁹

ZIFs are a class of MOFs where the metal atoms ($M^{n+} = Zn^{2+}, Co^{2+}$) are tetrahedrally coordinated to the N atoms of imidazolate derived linkers ($IM = C_3N_2H_3^-$) subtending an angle of 145° at the M-IM-M centre analogous to the Si-O-Si angle in zeolites to form porous architecture.¹⁰ They possess exceptional thermal and chemical stabilities

and exhibit diverse topologies. ZIF-8 ($Zn(mIM)_2$, mIM = 2-methyl imidazolate), a prototypical ZIF with sodalite (SOD) topology, crystallizes in cubic space group $I\bar{4}3m$ and exhibits a large solvent accessible volume (SAV) of 50%, making it an ideal candidate for studying the effect of pore occupancy on the mechanical properties and thus the guest-host interaction. ZIF-8 contains pores of 11.6 Å diameter connected by eight windows of 3.4 Å and its structure is flexible as evidenced by the adsorption of gases of kinetic diameter higher than its window dimensions (for example, N_2 and CH_4 of kinetic diameter greater than 3.6 Å).¹¹⁻¹³ At relatively high pressures (1.46 GPa), imidazolate linker rotates which increases the pore volume as well as window dimensions thus introducing more guest molecules inside the pores.¹⁴ This phase at high pressure has been called ZIF-8HP, while the one at ambient pressure is ZIF-8AP.¹² The enhanced gas uptake at low temperature is also explained by this gate opening. X ray diffraction (XRD), Fourier transform Infrared (FTIR), Raman and Nuclear magnetic resonance (NMR) experiments, etc have been employed to study the presence of guests with temperature or pressure.¹⁴⁻¹⁹

Brillouin spectroscopy has been used earlier to study the ambient temperature elastic properties of evacuated ZIF-8 which revealed its exceptionally low shear modulus.²⁰ Compared to ultrasonic and nanoindentation techniques, Brillouin spectroscopy is much more versatile, easy, and adaptable for many samples, making it an ideal tool to determine the acoustic velocity in MOFs. Moreover, temperature dependent adsorption studies can be carried out easily using Brillouin spectroscopy unlike nanoindentation.²¹ We have used Brillouin spectroscopy to study the effect of pore occupancy on the spectral features (the peak position,

^{a)} Author to whom correspondence should be addressed. Electronic mail: cbhas@jncasr.ac.in

width of the acoustic modes, and the central peak (CP)) of ZIF-8 by introducing various guests at room temperature. This is followed by the temperature dependence of acoustic modes upon gas adsorption.

II. EXPERIMENTAL METHODS

Brillouin spectra were recorded in backscattering geometry, using a 532 nm laser excitation with a power of 2 mW focused using a 20× objective lens. The scattered light was analyzed using a six pass tandem Fabry-Perot interferometer (JRS scientific instruments). Transmitted light was detected using a silicon photo avalanche diode (SPCM-AQR-16, Perkin Elmer, Canada) and processed by a multi-channel analyser with 1024 channels. A mirror spacing of 3.5 mm was used with a typical accumulation time of 5-10 min.

ZIF-8 was synthesised according to Ref. 10. All the reagents and solvents were used as supplied without further purification. 0.210 g of $\text{Zn}(\text{NO}_3)_2 \cdot 6\text{H}_2\text{O}$ and 0.06 g of 2-methyl imidazole (both obtained from Sigma-Aldrich) were mixed in 18 ml of *N,N*-dimethylformamide (DMF) and stirred for 20 min after which the mixture was heated at 140 °C for 24 h. On cooling the mixture, the mother liquid was removed and colourless polyhedral crystals (diameter ranging from 50 to 100 μm) were isolated. The crystals were then washed with DMF several times and immersed in methanol for solvent exchange, followed by heating at 150 °C for 6 h. The elastic property of ZIF-8 with respect to pore occupancy is studied by introducing various guests. Alcohols (methanol, ethanol, 1-propanol, and 1-butanol) and DMF were introduced by soaking ZIF-8 in respective solvents for 48 h after which they were taken in capillary tubes.

The temperature dependent gas adsorption measurements were done using a Linkam stage (THMS 600) with a temperature stability of 0.1 K. ZIF-8 crystals were enclosed between two coverslips with only the corners being sealed, letting sufficient gap for the gas to enter. Coverslips were used just to hold the sample, because cryogenic stage has to be placed vertically in our Brillouin setup. Heat transmitting grease was used to fix the coverslip on the stage. Prior to the experiment, sample was first heated to 120 °C for 1 h to remove any trapped solvent molecules and then cooled to room temperature. At this stage, gases (N_2 , CO_2 , and Ar) were introduced for 15 min, after which the sample was cooled at a rate of 10 °C/min, keeping the gas pressure at a constant value of ~ 1 atm.

III. RESULTS AND DISCUSSION

A typical Brillouin spectrum of evacuated ZIF-8 is shown in Fig. 1. Two acoustic modes are observed, namely, a longitudinal acoustic (LA) mode at ~ 16 GHz and a transverse acoustic (TA) mode at ~ 5 GHz. From the Brillouin study under ambient conditions by Tan *et al.*, we can say that the TA mode observed is the slow TA mode (TA1) which is related to the minimum value of shear modulus.²⁰ In addition to the acoustic modes, a quasielastic CP centered at zero frequency is also observed.

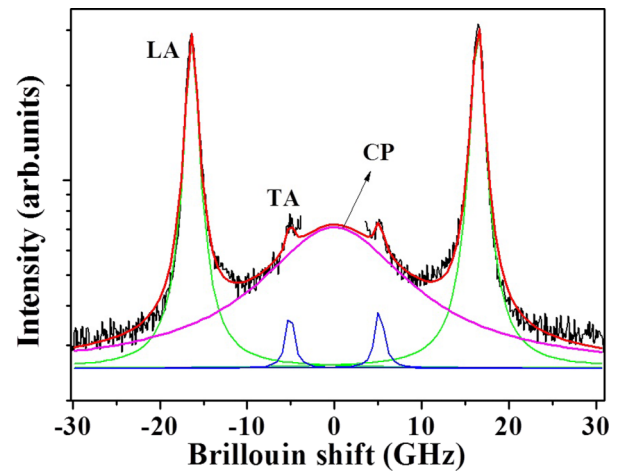


FIG. 1. Room temperature Brillouin spectra of evacuated ZIF-8 (LA—longitudinal acoustic mode, TA—transverse acoustic mode, and CP—central peak).

Brillouin spectra were obtained for samples of unknown crystallographic orientation and the acoustic velocity V can be determined from the Brillouin shift ν , using the relation $\nu = 2 \frac{2\pi}{\lambda} n V \sin \theta$, where n , λ , and θ are refractive index, excitation wavelength, and the scattering angle, respectively. The elastic properties can be derived from the direction dependence of the acoustic velocities which are obtained by rotating the sample along the azimuthal direction, ϕ considering a random direction (x) as $\phi = 0$ (Fig. 2(a)). We have used “envelop method” to determine the elastic constants from the ϕ dependence of Brillouin shifts. The envelop method is usually employed in deriving the elastic constants of the samples when the crystallographic orientation is unknown, especially in high pressure Brillouin experiments.^{22,23} In such cases, Brillouin shifts from many experimental runs are obtained and envelop of the data thus obtained are assumed to represent the maximum and minimum values of the shift. This method can be used even when a ϕ dependent study is not possible with the major disadvantage being the uncertainty in determining the extreme values of the Brillouin shift. Figure 2(b) shows the ϕ dependence of the LA and TA modes in evacuated ZIF-8 displaying the maxima and minima in the Brillouin shifts, which will occur along certain crystallographic directions. The Brillouin shift and FWHM (full width at half maximum) were obtained by fitting the LA, TA, and CP simultaneously using Lorentzian functions, as shown in Fig. 1. The independent elastic constants C_{11} , C_{12} , and C_{44} of ZIF-8 can be determined from the maximum and minimum values of acoustic modes and density (ρ) using the following relations:^{24–26}

$$V_{LA, max}^2 = C_{11}/\rho \text{ along } \langle 100 \rangle, \quad (1)$$

$$V_{LA, min}^2 = (C_{11} + 2C_{12} + 4C_{44})/3\rho \text{ along } \langle 111 \rangle, \quad (2)$$

$$V_{TA1, min}^2 = C_{44}/\rho. \quad (3)$$

The minimum value of TA1 (Eq. (3)) can be used to determine the minimum value of shear modulus, $G_{min} = C_{44}$ and the maximum value of LA determines C_{11} (Eq. (1)). Once C_{11} and C_{44} are known, C_{12} can be derived from the minimum

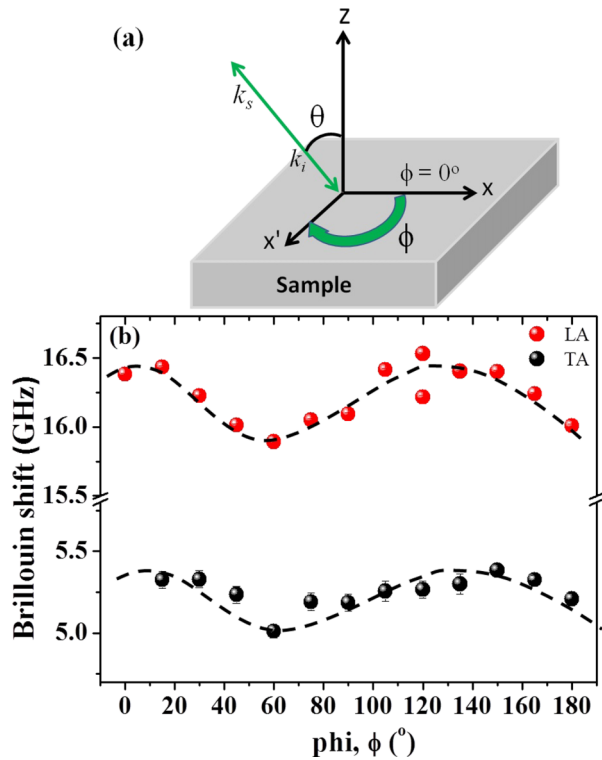


FIG. 2. (a) The schematic of the scattering geometry and phi dependent study on a ZIF-8 crystal. A random direction, x is taken as $\phi = 0^\circ$ and the sample is rotated azimuthally to a new direction x' . θ is the angle between the incident/scattered light (k_i/k_s) and the normal (z). (b) The phi dependence of LA and TA shift in evacuated ZIF-8 at room temperature. The dashed lines are guide to the eyes.

value of LA (Eq. (2)). The elastic constants C_{11} , C_{12} , and C_{44} thus obtained for evacuated ZIF-8 from our studies using a refractive index of 1.39 and density 950 kg/m^3 are 9.4, 6.7, and 0.90 GPa, respectively, which is in close agreement with the reported values of 9.52, 6.86, and 0.96 GPa.²⁰

A. Solvent incorporation at room temperature

The presence of solvent, its mass, and polarity can affect the elastic properties of guest-host systems. To calculate the acoustic velocities and elastic constants, the refractive index and density of solvent incorporated ZIF-8 is required. The effective refractive index of solvent incorporated ZIF-8 can be calculated using the formula $n_{\text{eff}} = \sqrt{V_{\text{sol}}n_{\text{sol}}^2 + V_{\text{fram}}n_{\text{fram}}^2 + (1 - V_{\text{fram}} - V_{\text{sol}})n_{\text{vac}}^2}$, where V_{sol} and V_{fram} are the volume fraction of the solvent and framework, respectively, and n_{sol} , n_{fram} , and n_{vac} are the refractive index of the solvent, framework, and vacuum, respectively. From the thermo gravimetric analysis (TGA, Fig. S2),²⁷ the number of molecules per unit cell determined for methanol, ethanol, propanol, butanol, and DMF incorporated ZIF-8 are 4, 4, 6, 8, and 7, respectively. These molecules occupy a volume fraction of approximately 0.1 within the framework. The density of solvent incorporated ZIF-8 can be obtained either from the literature or from the number of guest molecules determined using TGA. While the density of as-syn, evacuated, methanol, and butanol incorporated ZIF-8 can be obtained from the literature,^{10,14,20,28} some of the references have not taken into consideration the mass of the H atoms of the framework and the guests, for example, density of butanol incorporated ZIF-8.²⁸ Also, experimental conditions of Brillouin and density measurements (literature) are quite different. For example, in the case of methanol incorporated ZIF-8, density is obtained from the high pressure XRD experiment where the sample is surrounded by the methanol medium, while our Brillouin experiments are performed in the absence of liquid medium surrounding the sample. Thus, densities determined from the TGA measurements are more appropriate in determining the elastic constants. The effective refractive indices and the densities of the solvent incorporated ZIF-8 used in determining the elastic constants are given in Ref. 27. The Brillouin shifts, acoustic velocities, and elastic constants of solvent incorporated and evacuated ZIF-8 are given in Table I.

TABLE I. Acoustic and elastic properties of evacuated and solvent incorporated ZIF-8 at 298 K. The first line in the acoustic velocities and elastic constants of each sample corresponds to the values determined using the density and pore occupancy obtained from the literature, while the second line corresponds to the same determined from our experiments.

Sample	LA (max/min) (GHz)	TA (min) (GHz)	FWHM-LA (GHz)	$V_{\text{max}}/V_{\text{min}}$ ($\pm 0.006 \text{ km/s}$)	C_{11} ($\pm 0.04 \text{ GPa}$)	C_{12} ($\pm 0.03 \text{ GPa}$)	C_{44} ($\pm 0.01 \text{ GPa}$)	CP ($\pm 2 \text{ GHz}$)
As-syn	17.11/16.89	5.22	1.833 ± 0.12	3.072/3.051 3.173/3.134	10.77 11.48	8.37 8.93	1.00 1.07	13
DMF	17.87/17.60	5.28	2.05 ± 0.12	3.209/3.179 3.314/3.265	11.75 12.05	9.18 9.42	1.03 1.05	13
Methanol	16.43/16.25	5.14	0.99 ± 0.08	3.002/2.936 3.087/3.051	9.52 9.22	7.33 7.11	0.93 0.90	12.5
Ethanol	16.58/16.41	5.02	0.91 ± 0.06	3.013/2.964 3.102/3.077	... 9.41	... 7.45	... 0.87	7.4
1-propanol	16.31/16.18	5.21	1.4 ± 0.07	2.954/2.923 3.047/3.027	... 9.74	... 7.53	... 0.93	8
1-butanol	16.37/16.19	5.14	1.33 ± 0.08	2.959/2.925 3.039/3.025	9.77 10.38	7.51 8.16	0.96 1.04	9
Evacuated	16.43/15.89	5.06	1.258 ± 0.14	3.145/2.871 3.145/3.041	9.39 9.15	6.71 6.52	0.90 0.87	17
Evacuated ^a	3.17/3.08	9.52	6.86	0.96	...

^aReference 20.

The error in the Brillouin shifts was determined using the procedure given in Ref. 29 using a standard deviation of ~ 0.05 GHz (shifts given in Table I are the mean from 6 data) and an instrumental resolution of ~ 0.08 GHz.

The decrease in the Brillouin shift of as-syn ZIF-8 on evacuation indicates the role of guest molecules in strengthening the framework as predicted by Ortiz *et al.*³⁰ Upon re-adsorption of DMF, the observed shift is higher than that of as-syn ZIF-8, probably because as-syn ZIF-8 has both DMF and water molecules inside, while on re-adsorption only DMF molecules are present.¹⁰ This demonstrates the permanent porosity character of ZIF-8 as well as the nature of the guest in determining the elastic properties of the framework. This also gives the evidence for the presence of guest molecules in the pores and its interaction with the framework.

For alcohol incorporated ZIF-8, on increasing the chain length, the acoustic velocity decreases. The elastic constants increase as n increases from 1 to 4 with DMF incorporated ZIF-8 (DMF@ZIF-8) exhibiting the highest elastic constants. On introducing solvents, C_{12} exhibits a huge increase when compared to other elastic constants as it increases by approximately 44% and 25% for DMF@ZIF-8 and butanol incorporated ZIF-8 (butanol@ZIF-8), respectively, when compared to the evacuated ZIF-8. ZIF-8 is elastically anisotropic²⁰ with the maximum value of Young's modulus (E) along $\langle 100 \rangle$ direction and minimum along $\langle 111 \rangle$ direction. The Young's modulus determined along these directions is shown in Table II.²⁵ It can be observed that $E \langle 111 \rangle$ increases on incorporating solvents, which can be accredited to the increase in C_{12} . The $\langle 111 \rangle$ direction is normal to the six-membered rings of ZIF-8²⁰ which is a major guest occupation site.^{19,31} An increase in $E \langle 111 \rangle$ thus gives an indirect evidence for the guest adsorption near the six-membered rings of ZIF-8. Also the difference between $E \langle 100 \rangle$ and $E \langle 111 \rangle$ decreases on incorporating the guests which indicates a decrease in the anisotropy of the Young's modulus.

The XRD studies in methanol and butanol incorporated ZIF-8 have shown that there are 12 molecules of each per unit cell.^{14,28} Assuming that ethanol and propanol incorporated ZIF-8 also have 12 molecules per unit cell, elastic constants determined will increase on increasing the chain length which implies that the trend in the elastic constants will not change

TABLE II. The maximum and minimum values of the Young's modulus (E) which occur along the $\langle 100 \rangle$ and $\langle 111 \rangle$ directions, respectively, for solvent incorporated and evacuated ZIF-8. The elastic constants derived using the density obtained from TGA measurements are used for calculating E .

Sample	$E \langle 100 \rangle$ (± 0.02 GPa)	$E \langle 111 \rangle$ (± 0.02 GPa)
As-syn	3.68	3.04
DMF	3.79	3.00
Methanol	3.04	2.55
Ethanol	2.83	2.46
1-propanol	3.13	2.81
1-butanol	3.19	2.93
Evacuated	3.73	2.45
Evacuated ^a	3.77 ± 0.01	2.78 ± 0.01

^aReference 20.

even if experimental values of the density are used, though their values may differ.

The decrease in the acoustic velocity on increasing the chain length of alcohols is similar to the behaviour exhibited by the clathrates and can be explained as a result of the stiffening of the framework due to the guest-host interaction.³² Mass and number of butanol and DMF molecules incorporated in ZIF-8 are almost the same but the difference in the values of their elastic constants shows that interaction between framework and guest indeed affects the elastic constants. DMF possesses the highest polarizability among the solvents used. Also, it is shown from DFT calculations that the interaction between the ZIF-8 and alcohol increases as we go from methanol to butanol so are their polarisabilities.³³ Thus, elastic constants increase as the polarizability of guest in ZIF-8 is increased. A high filling of the cage by the guests can also increase the elastic constants as it can buttress the cage larger. Thus, the guest-host interaction as well as filling factor/high packing affects the elastic constants.^{34,35}

On increasing the chain length, FWHM of the LA also increases and DMF@ZIF-8 exhibits the maximum FWHM. A high FWHM of LA indicates a high attenuation coefficient or a low phonon life-time which indicates high phonon scattering due to the guest-host interaction. Thus, an increase in the FWHM implies that the guest molecules can absorb and scatter the phonons by the coupling of vibrational modes of guest molecules with the acoustic modes of host.^{32,36} Such changes in the FWHM result in low thermal conductivity in guest-host systems as exemplified by clathrate hydrates.³² Unlike in the case of clathrate hydrate, we observe that the thermal conductivity of the evacuated ZIF-8 (higher FWHM) is lower than that when the guest molecules are incorporated into the ZIF-8 (lower FWHM). This is because the guest molecules can hop between the cages adding to the thermal conductivity. The bulkier the guest molecule, the lower the thermal conductivity (higher FWHM). The changes in FWHM in our study indicate that we can tune the thermal conductivity of ZIF-8 by incorporation of solvents.

It has to be mentioned that while obtaining the Brillouin spectrum, if we have excess solvent surrounding the ZIF-8 and a strong LA mode of the solvent is observed in the spectrum, the average value of LA shift and FWHM of ZIF-8 is ~ 17 GHz and ~ 1.4 GHz, respectively, irrespective of the solvent incorporated. Moreover, the LA mode of the solvent makes it difficult to observe the weak TA mode of ZIF-8 as the Brillouin shift of solvent overlaps with the TA of ZIF-8 (LA mode is at 8.1 GHz for DMF and for alcohols, it increases from 5.6 to 6.8 GHz as the chain length is increased). To circumvent this problem, we have performed our Brillouin experiments after removing the extra solvent molecules by heating the capillary tube, so that LA of the solvent vanishes and TA of the ZIF-8 appears. In order to confirm that the solvent is present within the ZIF-8 after this process, we have performed the TGA and FTIR experiments.²⁷ A strong peak at 1680 cm^{-1} in the FTIR spectrum indicates the presence of DMF in as-synthesised ZIF-8, while O-H stretching peaks ascertain the presence of alcohol (in alcohol incorporated ZIF-8) and water (in as-synthesised ZIF-8¹⁰).²⁷ The high value of Brillouin shift exhibited by ZIF-8 when the liquid

medium surrounds ZIF-8 (i.e., LA of the solvents are present) compared to the case when the extra liquid is removed (shown in Table I) could be probably due to the hyper-saturation of the pores of ZIF-8 by the solvent. Using the density of the methanol incorporated framework obtained from the high pressure XRD¹⁴ measurements and the density of butanol incorporated ZIF-8,²⁸ the elastic constant C_{11} determined from a Brillouin shift of 17 GHz for methanol as well as butanol incorporated ZIF-8 is ~ 9.9 GPa and 11.1 GPa, respectively, which again follows the trend of increase in the elastic constants on increasing the chain length.

B. Gas adsorption

We now focus on the temperature dependent gas adsorption studies. Ideally, to determine the elastic constants, one has to study the ϕ dependence of the LA and TA modes. In our setup, we cannot study the ϕ dependence of these crystals inside the cryogenic stage and hence, the elastic constants could not be directly determined. On introducing guests, the difference between the maximum and minimum values of Brillouin shift of LA mode decreases (see Table I). Considering the velocities obtained as $V_{LA,max}$ and $V_{TA,min}$, the elastic constants C_{11} and C_{44} can be obtained, even though the values thus determined will have an error of $\sim 2\%$ – 3% . Hence, the changes in LA and TA can be correlated as the changes in C_{11} and the shear modulus C_{44} , respectively.

The average value of Brillouin shift decreases upon exposing to various gases. At 298 K, a gas pressure of 1 atm results in the decrease of TA and LA shifts by $\sim 5\%$ and 3% , respectively, independent of the gas, implying that TA modes are more pliable.²⁷ The decrease in the Brillouin shift could be due to the increase in the cell and pore volume pertaining to the intake of gas, analogous to the high pressure experiments.¹⁴ Raman experiments done under similar conditions did not show any change on guest incorporation implying that the pore occupancy plays a significant role in the mechanical properties of ZIF-8 and the microscopic properties are unaltered.

Temperature dependent Brillouin shift and FWHM of LA mode for nitrogen adsorption are shown in Figs. 3(a) and 3(b). Both shift and FWHM show significant changes near 260 K and 150 K. The changes near 260 K probably indicate the onset of significant gas uptake, as at the room temperature, only a few molecules will be adsorbed,^{12,37} while the changes at 150 K are attributed to the rotation of the methyl-imidazolate linker which further increases the amount of gas adsorbed. Temperature dependent Raman studies show that major changes occur in imidazolate ring puckering mode upon adsorbing gases¹⁷ since the gas molecules are adsorbed near the imidazolate linkers. Imidazolate ring puckering mode also shows significant changes at 260 K and 150 K,²⁷ which demonstrates the role of the imidazolate linker in determining the elastic properties of ZIFs as well as the ability of Brillouin spectroscopy for capturing the flexibility of ZIF-8. The imidazolate ligands determine the stiffness in ZIFs as a bulkier linker results in higher stiffness.⁹ The changes in the LA shift observed here illustrate the dependence of elastic constants, particularly C_{11} , on the imidazolate linker as it becomes bulkier upon adsorbing gas.

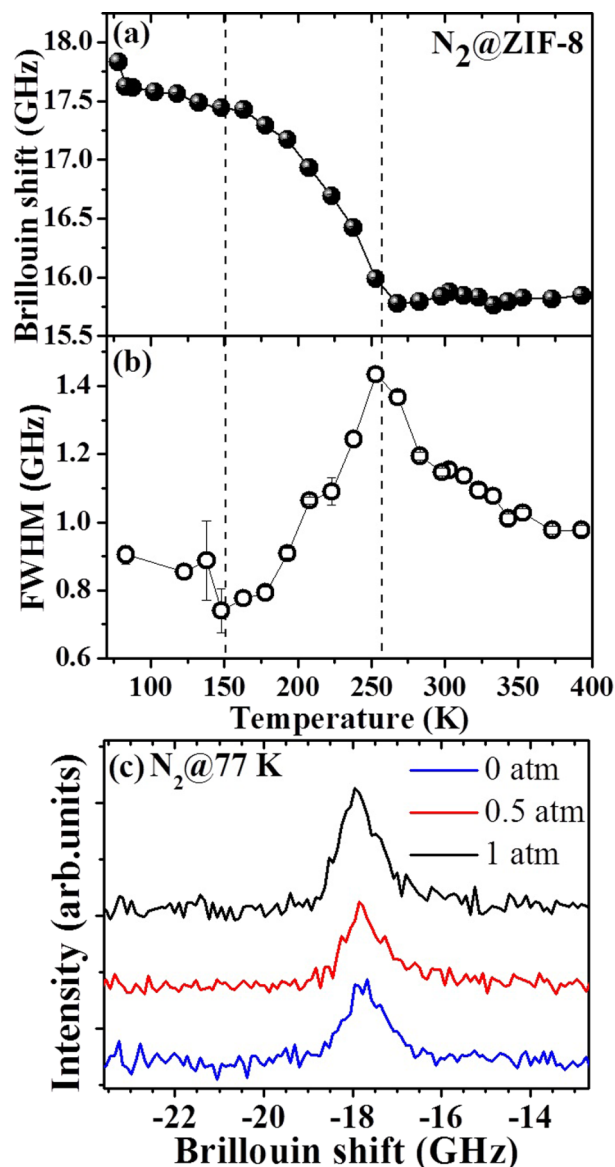


FIG. 3. Temperature dependence of (a) Brillouin shift and (b) FWHM of the LA mode during nitrogen adsorption. (c) The Brillouin spectra of LA mode at 77 K and varying N₂ gas pressures. From the adsorption isotherm, N₂ gas adsorbed by ZIF-8 corresponds to 0, 125, and 350 ml g⁻¹ at 0, 0.5, and 1 atm, respectively.¹⁷

During temperature dependent gas adsorption studies, temperature and gas uptake change simultaneously. Incorporating guests increase the elastic properties in many porous materials, zeolites, and ZIF-8,^{30,35,38,39} while decreasing the temperature can also increase the elastic constants due to the increase in the bond strength. To separate the effects due to temperature and guest uptake, Brillouin experiments were performed at a constant temperature and varying gas pressures. The Brillouin spectra obtained at 77 K on increasing the N₂ gas pressure (0, 0.5, and 1 atm) are given in Fig. 3(c). The adsorption isotherm at 77 K from Ref. 17 shows that the amount of N₂ gas adsorbed by ZIF-8 corresponds 0, 125, and 350 ml g⁻¹ at 0, 0.5, and 1 atm, respectively, indicating that the number of gas molecules adsorbed by the framework increases on increasing the gas pressure. But Brillouin shift increases by only ~ 0.1 GHz on increasing the gas pressure

from 0 to 1 atm. From the XRD measurements, the density of N₂ incorporated ZIF-8 corresponds to 1383 kg/m³ (56 N₂ molecules per unit cell).¹⁹ On the assumption that the LA observed is LA_{max}, the elastic constant C₁₁ estimated for 0 and 1 atm N₂ corresponds to 10.4 GPa and 15.5 GPa, respectively. At room temperature, C₁₁ is 9.1 GPa for an evacuated ZIF-8 and hence, the isothermal studies of elastic constants show that temperature as well as the guest uptake effects the elastic constants with the guest incorporation being the dominant factor for increasing the elastic constants.

Figure 4(a) shows the percentage of Brillouin shift of LA mode versus temperature for N₂, CO₂, and Ar adsorption. The temperature dependence was the same for all the gases adsorbed up to 225 K, below which their behaviour deviates. Nitrogen adsorbed ZIF-8 (N₂@ZIF-8) and argon adsorbed ZIF-8 (Ar@ZIF-8) show changes near 260 K and 150 K pertaining to the beginning of significant gas uptake and gate opening, but interestingly shift of Ar@ZIF-8 saturates at a slightly lower value than N₂@ZIF-8. The Brillouin shift of carbon dioxide adsorbed ZIF-8 (CO₂@ZIF-8) increases steeply below 225 K and it does not show any saturation behaviour, unlike N₂@ZIF-8 and Ar@ZIF-8. The saturation could not be studied here for CO₂@ZIF-8 below the gate opening as CO₂ solidifies around 195 K. Gas adsorption depends upon the size, shape, and polarity of the guest molecules and all the gases are adsorbed near the imidazolate ligands regardless of the nature of gas.^{11,40,41} At 210 K, the LA shift decreases as the polarizability of the gas is decreased (i.e., shift decreases in the order CO₂ > N₂ > Ar) similar to the case of solvent incorporation.

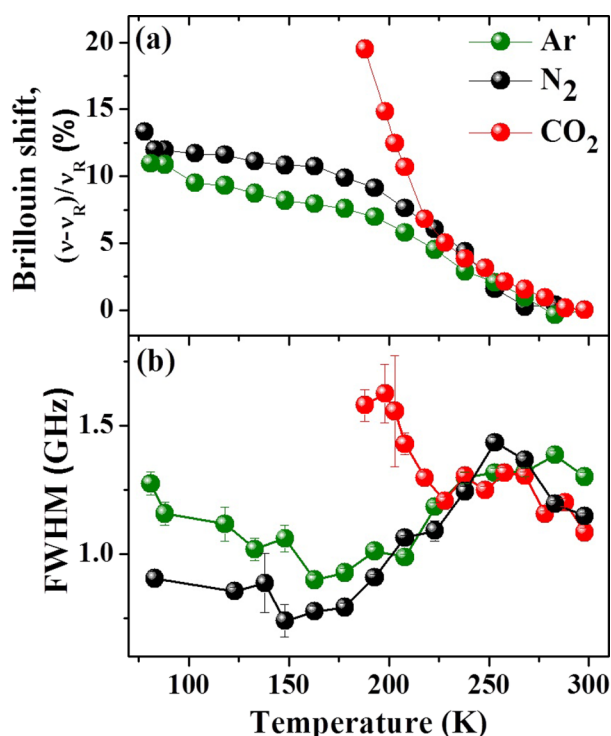


FIG. 4. Temperature dependence of (a) Brillouin shift and (b) FWHM of LA mode during CO₂, N₂, and Ar adsorption.

All the gases follow a similar trend in FWHM up to 225 K, though the peak at 260 K is not clearly observable for Ar adsorption (Fig. 4(b)). Below 230 K, FWHM for CO₂@ZIF-8 is seen to increase steeply, similar to N₂ and Ar adsorption beyond 150 K. Since the FWHM can be also an indicator of interactions between framework and guest as observed from our solvent incorporation studies and also due to polarizability. In the case of CO₂, we observe an abrupt increase in the LA mode frequency and the FWHM. This is because when the gate opening is approaching, there is an influx of CO₂ molecules into the framework but it is also close to solidification temperature. Due to the high polarizability of CO₂ molecule as well as lower dynamics of the gas due to approaching solidification, there is a strong interaction between the framework and the gas molecules of CO₂. This leads to an abrupt increase in the LA frequency as well as due to strong interactions between the framework and the guest molecule; the phonon lifetime is shorter leading to higher FWHM. On the other hand, N₂ and Ar have similar polarisabilities and show much reduced effect on FWHM and the minor changes between the two are within the experimental error bar.

Figure 5 depicts the temperature dependence of TA mode of N₂@ZIF-8. Brillouin shift of TA decreases slightly as the temperature is decreased and then steeply increases below 260 K as significant gas adsorption commences, similar to the behaviour of LA mode. Irrespective of the gases adsorbed, the temperature dependence of TA shows similar behaviour up to 200 K, (inset of Figure 5) below which the TA modes disappeared. At 220 K, the percentage Brillouin shift exhibited by TA modes is ~10%, whereas the LA modes exhibit only a 5% change. This implies that the rigidity of framework against elastic distortions arising from external shear loading undergoes a huge increase on decreasing the temperature.²⁰ Shear modulus of ZIF-8 which is the lowest observed under ambient conditions among extended solids decreases on decreasing the temperature and increases on adsorbing gas.²⁰ Though the elastic constants change on decreasing the temperature, the Born stability conditions^{30,42} will be satisfied under all the experimental conditions investigated implying the mechanical stability of guest incorporated ZIF-8.

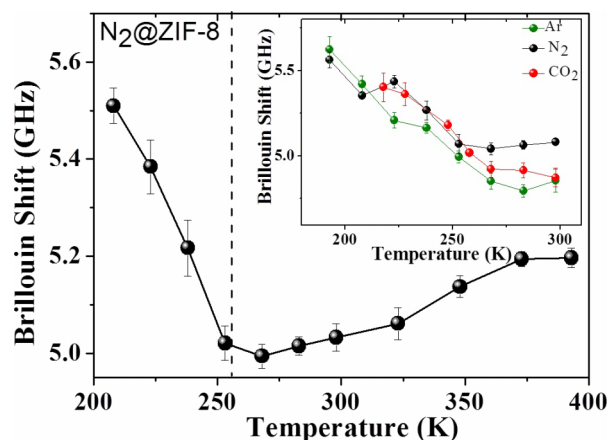


FIG. 5. Temperature dependence of TA1 for N₂ adsorption. Inset shows the dependence for all the gases studied.

C. Central peak

The CP (Figure 1) also shows changes on guest incorporation (Table I) and temperature. We could not determine the difference in FWHM of CP for $n = 2-4$ alcohols as fitting of CP is prone to an error of ± 2 GHz. The CP can originate due to three factors: it can be (1) intrinsic to the sample, (2) intrinsic to the guest molecules, or (3) due to the motion of the guest molecules within the framework.

CP intrinsic to the sample: FWHM of CP is related to the thermal diffusivity, D_{th} by the relation $2D_{th}q^2 = \Gamma$, where $D_{th} = \frac{1}{3}V_D l$. Here, q is the phonon wave vector, Γ is FWHM, V_D is the average velocity, and l is the mean free path.^{43,44} The mean free path of phonons in ZIF-8 ranges from 1.7 to 3.5 nm.⁴⁵ Assuming an average velocity of 1300 m/s, $D_{th} = 1.1 \times 10^{-6}$ m²/s corresponding to a FWHM of ~ 0.4 GHz. Thus, FWHM of the CP observed in our experiments cannot be attributed to the thermal conductivity of ZIF-8.

CP intrinsic to the guest molecules: Gases and liquids undergo various relaxation processes and exhibit CP in their Brillouin spectra. The CP due to the thermal fluctuations of gas molecules will be very narrow (FWHM ~ 1 GHz)^{46,47} and that of solvent molecules will be very weak as even the LA modes of solvents are not observable in the Brillouin spectra.⁴⁸ Thus, CP observed cannot be attributed to the intrinsic relaxation of guest molecules. Hence, we believe that CP originates due to the motion of the guest molecules within the framework and its interaction with the framework. Guest molecules can undergo two kinds of motions, whereby it can interact with the MOF. The guest molecules can hop from one pore to another through the connecting windows or it can collide with the pore walls of the ZIF-8 and move within the cage.⁴⁹ Using the FWHM (Γ) of the central peak, relaxation time can be derived from the relation $\tau = 1/\pi\Gamma$. Relaxation times thus obtained for evacuated (as well as gas adsorbed), methanol, and butanol incorporated ZIF-8 are 18, 25, and 35 ps, respectively. The FWHM (~ 17 GHz) and hence the relaxation time obtained for evacuated and gas adsorbed ZIF-8 are similar because Brillouin experiments were not performed under vacuum conditions and evacuated ZIF-8 was exposed to air after evacuation. Assuming a diffusivity of $\sim 10^{-10}$ m²/s for CO₂ in ZIF-8, we derive a relaxation time of ~ 20 ps using the formula $D = a^2/6\tau$, where a can be approximated as ~ 1 Å^{50,51} which is in agreement with the relaxation time obtained from our Brillouin spectra. But the relaxation time obtained from CP is agreeable with the calculated values only in the case of gases where diffusivity is of the order of 10^{-9} – 10^{-10} m²/s. For alcohols, the self diffusivity ranges from 10^{-11} to 10^{-16} m²/s which is lower than the gases and it reduces as n is increased.⁵²⁻⁵⁴ Moreover, for the solvents (unlike gases), the factors like adsorbate-adsorbate interactions and clustering⁵⁵ become significant which make it difficult to assign the CP to intercage hopping motion; however, it is certain that the CP is indeed due to the motion of the guest molecules.

CP broadened and its intensity became very weak below 160 K during the gas adsorption studies (Fig. 6). In porous materials with windows, dimension of window have a huge impact on the diffusivity of the guest. The sudden broadening

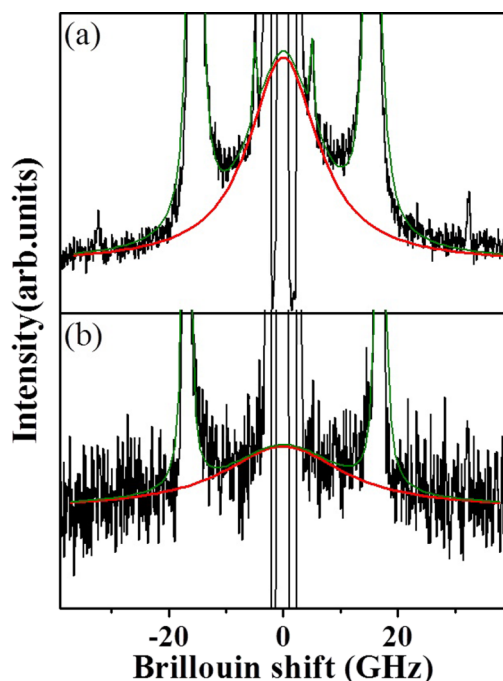


FIG. 6. The central peak (shown by red curve) observed during Ar adsorption studies in ZIF-8 at (a) 293 K and (b) 103 K. The spectrum in (b) has been enlarged by a factor of 5.

of the CP in ZIF-8HP phase thus indicates an increase in the diffusivity of the guest molecules as the window size enlarges.^{12,55} This observation again proves that CP originates due to the motion of the guest molecules within the framework.

IV. CONCLUSIONS

In conclusion, the effect of pore occupancy on the elastic properties of ZIF-8 has been studied by introducing various guests. The polarizability of the guests affects the elastic properties, lifetime, and the guest dynamics inside the pores. The behaviour of the elastic constants suggests a decrease in the elastic anisotropy of ZIF-8 upon guest incorporation. The flexibility of ZIF-8 on gas adsorption was captured from the changes in the Brillouin shift and FWHM of the LA mode. On decreasing the temperature, we observe a large increase in shear modulus compared to the increase in the Young's modulus. The high shear stiffening observed at low temperatures can circumvent the shear induced amorphisation of ZIF-8 observed earlier. This could potentially catalyze the industrial applications of ZIF-8.

ACKNOWLEDGMENTS

D.R. thanks UGC for funding and Venkata Srinu Bhadrani and Gayatri Kumari for fruitful discussions.

¹P. Horcajada, R. Gref, T. Baati, P. K. Allan, G. Maurin, P. Couvreur, G. Férey, R. E. Morris, and C. Serre, *Chem. Rev.* **112**, 1232 (2012).

²H. C. Zhou, J. R. Long, and O. M. Yaghi, *Chem. Rev.* **112**, 673 (2012).

³J. C. Tan and A. K. Cheetham, *Chem. Soc. Rev.* **40**, 1059 (2011).

⁴F. X. Coudert, A. Boutin, A. H. Fuchs, and A. V. Neimark, *J. Phys. Chem. Lett.* **4**, 3198 (2013).

⁵S. S. Han and W. A. Goddard, *J. Phys. Chem. C* **111**, 15185 (2007).

- ⁶T. D. Bennett, J. Sotelo, J. C. Tan, and S. A. Moggach, *CrystEngComm* **17**, 286 (2015).
- ⁷P. Canepa, K. Tan, Y. Du, H. Lu, Y. J. Chabal, and T. Thonhauser, *J. Mater. Chem. A* **3**, 986 (2015).
- ⁸S. Henke, W. Li, and A. K. Cheetham, *Chem. Sci.* **5**, 2392 (2014).
- ⁹J. C. Tan, T. D. Bennett, and A. K. Cheetham, *Proc. Natl. Acad. Sci. U. S. A.* **107**, 9938 (2010).
- ¹⁰K. S. Park, Z. Ni, A. P. Côté, J. Y. Choi, R. Huang, F. J. Uribe-Romo, H. K. Chae, M. O'Keeffe, and O. M. Yaghi, *Proc. Natl. Acad. Sci. U. S. A.* **103**, 10186 (2006).
- ¹¹C. O. Ania, E. García-Pérez, M. Haro, J. J. Gutiérrez-Sevillano, T. Valdés-Solís, J. B. Parra, and S. Calero, *J. Phys. Chem. Lett.* **3**, 1159 (2012).
- ¹²D. Fairen-Jimenez, S. A. Moggach, M. T. Wharmby, P. A. Wright, S. Parsons, and T. Düren, *J. Am. Chem. Soc.* **133**, 8900 (2011).
- ¹³H. Tanaka, S. Ohsaki, S. Hiraide, D. Yamamoto, S. Watanabe, and M. T. Miyahara, *J. Phys. Chem. C* **118**, 8445 (2014).
- ¹⁴S. A. Moggach, T. D. Bennett, and A. K. Cheetham, *Angew. Chem.* **121**, 7221 (2009).
- ¹⁵Y. Hu, H. Kazemian, S. Rohani, Y. Huang, and Y. Song, *Chem. Commun.* **47**, 12694 (2011).
- ¹⁶Y. Hu, Z. Liu, J. Xu, Y. Huang, and Y. Song, *J. Am. Chem. Soc.* **135**, 9287 (2013).
- ¹⁷G. Kumari, K. Jayaramulu, T. K. Maji, and C. Narayana, *J. Phys. Chem. A* **117**, 11006 (2013).
- ¹⁸M. A. Springuel-Huet, A. Nossou, F. Guenneau, and A. Gedeon, *Chem. Commun.* **49**, 7403 (2013).
- ¹⁹J. P. Zhang, A. X. Zhu, and X. M. Chen, *Chem. Commun.* **48**, 11395 (2012).
- ²⁰J. C. Tan, B. Civalieri, C. C. Lin, L. Valenzano, R. Galvelis, P. F. Chen, T. D. Bennett, C. Mellot-Draznieks, C. M. Zicovich-Wilson, and A. K. Cheetham, *Phys. Rev. Lett.* **108**, 095502 (2012).
- ²¹U. Ramamurty and J.-i. Jang, *CrystEngComm* **16**, 12 (2014).
- ²²M. Grimsditch, P. Loubeyre, and A. Polian, *Phys. Rev. B* **33**, 7192 (1986).
- ²³H. Shimizu, H. Tashiro, T. Kume, and S. Sasaki, *Phys. Rev. Lett.* **86**, 4568 (2001).
- ²⁴W. F. Hosford, *Mechanical Behavior of Materials* (Cambridge University Press, New York, 2005).
- ²⁵R. E. Newnham, *Properties of Materials* (Oxford University Press, Inc., New York, NY, 2005).
- ²⁶R. L. W. Hayes, *Scattering of Light by Crystals* (John Wiley & Sons, New York, 1978).
- ²⁷See supplementary material at <http://dx.doi.org/10.1063/1.4937763> for synthesis, characterisation of ZIF-8, Brillouin experiment, Raman spectroscopy, temperature dependence of central peak, and properties of guest incorporated ZIF-8.
- ²⁸J. C. S. Remi, T. Rémy, V. Van Hunskerken, S. van de Perre, T. Duerinck, M. Maes, D. De Vos, E. Gobechiya, C. E. A. Kirschhock, G. V. Baron, and J. F. M. Denayer, *ChemSusChem* **4**, 1074 (2011).
- ²⁹L. Kirkup, *Data Analysis for Physical Scientists* (Cambridge University Press, New York, 2012).
- ³⁰A. U. Ortiz, A. Boutin, A. H. Fuchs, and F.-X. Coudert, *J. Phys. Chem. Lett.* **4**, 1861 (2013).
- ³¹D. Fairen-Jimenez, R. Galvelis, A. Torrisi, A. D. Gellan, M. T. Wharmby, P. A. Wright, C. Mellot-Draznieks, and T. Duren, *Dalton Trans.* **41**, 10752 (2012).
- ³²H. Kieft, M. J. Clouter, and R. E. Gagnon, *J. Phys. Chem.* **89**, 3103 (1985).
- ³³K. Zhang, L. Zhang, and J. Jiang, *J. Phys. Chem. C* **117**, 25628 (2013).
- ³⁴C. A. Sandstedt, D. Michalski, and C. J. Eckhardt, *J. Chem. Phys.* **112**, 7606 (2000).
- ³⁵L. Bouéssel du Bourg, A. U. Ortiz, A. Boutin, and F.-X. Coudert, *APL Mater.* **2**, 124110 (2014).
- ³⁶J. S. Tse, M. L. Klein, and I. R. McDonald, *J. Chem. Phys.* **81**, 6146 (1984).
- ³⁷H. Huang, W. Zhang, D. Liu, B. Liu, G. Chen, and C. Zhong, *Chem. Eng. Sci.* **66**, 6297 (2011).
- ³⁸R. Arletti, L. Leardini, G. Vezzalini, S. Quartieri, L. Gigli, M. Santoro, J. Haines, J. Rouquette, and L. Konczewicz, *Phys. Chem. Chem. Phys.* **17**, 24262 (2015).
- ³⁹B. Coasne, J. Haines, C. Levelut, O. Cambon, M. Santoro, F. Gorelli, and G. Garbarino, *Phys. Chem. Chem. Phys.* **13**, 20096 (2011).
- ⁴⁰Y. Liu, H. Liu, Y. Hu, and J. Jiang, *J. Phys. Chem. B* **114**, 2820 (2010).
- ⁴¹J. Pérez-Pellitero, H. Amrouche, F. R. Siperstein, G. Pirngruber, C. Nieto-Draghi, G. Chaplais, A. Simon-Masseron, D. Bazer-Bachi, D. Peralta, and N. Bats, *Chem.–Eur. J.* **16**, 1560 (2010).
- ⁴²G. Grimvall, B. Magyari-Köpe, V. Ozoliņš, and K. A. Persson, *Rev. Mod. Phys.* **84**, 945 (2012).
- ⁴³A. Koreeda, T. Nagano, S. Ohno, and S. Saikan, *Phys. Rev. B* **73**, 024303 (2006).
- ⁴⁴A. Koreeda, R. Takano, and S. Saikan, *Phys. Rev. B* **80**, 165104 (2009).
- ⁴⁵X. Zhang and J. Jiang, *J. Phys. Chem. C* **117**, 18441 (2013).
- ⁴⁶T. J. Greytak and G. B. Benedek, *Phys. Rev. Lett.* **17**, 179 (1966).
- ⁴⁷R. P. Sandoval and R. L. Armstrong, *Phys. Rev. A* **13**, 752 (1976).
- ⁴⁸J. H. Ko and S. Kojima, *J. Korean Phys. Soc.* **39**, 702 (2001).
- ⁴⁹D. I. Kolokolov, L. Diestel, J. Caro, D. Freude, and A. G. Stepanov, *J. Phys. Chem. C* **118**, 12873 (2014).
- ⁵⁰L. Zhang, G. Wu, and J. Jiang, *J. Phys. Chem. C* **118**, 8788 (2014).
- ⁵¹R. A. Field, D. A. Gallagher, and M. V. Klein, *Phys. Rev. B* **18**, 2995 (1978).
- ⁵²C. Chmelik, H. Bux, J. Caro, L. Heinke, F. Hibbe, T. Titze, and J. Kärger, *Phys. Rev. Lett.* **104**, 085902 (2010).
- ⁵³J. A. Gee, J. Chung, S. Nair, and D. S. Sholl, *J. Phys. Chem. C* **117**, 3169 (2013).
- ⁵⁴K. Zhang, R. P. Lively, C. Zhang, R. R. Chance, W. J. Koros, D. S. Sholl, and S. Nair, *J. Phys. Chem. Lett.* **4**, 3618 (2013).
- ⁵⁵R. Krishna, *Chem. Soc. Rev.* **41**, 3099 (2012).